

RESEARCH

Open Access



# Integrated analysis identifies oxidative stress-related lncRNAs associated with progression and prognosis in colorectal cancer

Rui Chen and Jun-Min Wei\*

\*Correspondence:  
weijunmin@sdu.edu.cn

Department of Oncology, Qilu  
Hospital, Cheeloo College  
of Medicine, Shandong  
University, Jinan, China

## Abstract

**Background:** Colorectal cancer (CRC) is one of the most common cancers in the world. Oxidative stress reactions have been reportedly associated with oncogenesis and tumor progression. By analyzing mRNA expression data and clinical information from The Cancer Genome Atlas (TCGA), we aimed to construct an oxidative stress-related long noncoding RNA (lncRNA) risk model and identify oxidative stress-related biomarkers to improve the prognosis and treatment of CRC.

**Results:** Differentially expressed oxidative stress-related genes (DEOSGs) and oxidative stress-related lncRNAs were identified by using bioinformatics tools. An oxidative stress-related lncRNA risk model was constructed based on 9 lncRNAs (*AC034213.1*, *AC008124.1*, *LINC01836*, *USP30-AS1*, *AP003555.1*, *AC083906.3*, *AC008494.3*, *AC009549.1*, and *AP006621.3*) by least absolute shrinkage and selection operator (LASSO) analysis. The patients were then divided into high- and low-risk groups based on the median risk score. The high-risk group had a significantly worse overall survival (OS) ( $p < 0.001$ ). Receiver operating characteristic (ROC) and calibration curves displayed the favorable predictive performance of the risk model. The nomogram successfully quantified the contribution of each metric to survival, and the concordance index and calibration plots demonstrated its excellent predictive capacity. Notably, different risk subgroups showed significant differences in terms of their metabolic activity, mutation landscape, immune microenvironment and drug sensitivity. Specifically, differences in the immune microenvironment implied that CRC patients in certain subgroups might be more responsive to immune checkpoint inhibitors.

**Conclusions:** Oxidative stress-related lncRNAs can predict the prognosis of CRC patients, which provides new insight for future immunotherapies based on potential oxidative stress targets.

**Keywords:** Oxidative stress, lncRNA, Colorectal cancer, Immunotherapy



## Background

Colorectal cancer (CRC) is the third most common malignancy worldwide accounting for 9% of all cancer cases, and the fourth most common cause of cancer-related deaths [1]. The combination of folinic acid, 5-fluorouracil, oxaliplatin and/or irinotecan are the efficacious chemotherapy drugs for CRC. In addition, the use of monoclonal antibodies against vascular endothelial growth factor and epidermal growth receptor increased the efficiency of chemotherapy regimens and the survival time of CRC patients, but most patients develop resistance to drugs over a longer course of treatment [2]. Immunotherapy is another promising treatment for CRC, and a growing number of immunotherapy drugs are currently being developed, which can potentially increase treatment effectiveness and reduce side effects [3].

Many risk factors, including environmental factors, smoking, alcohol consumption, diet and obesity, are related to the onset and progression of CRC [4]. The cross talk between these known risk factors can lead to oxidative stress and the overproduction of reactive oxygen species (ROS) in cells, which can gradually result in gene mutations and promote tumor initiation [5–7]. It can also promote tumor growth by activating the receptor tyrosine kinase (RTK), phosphatidylinositol 3-kinase (PI3K)/Akt, and nuclear factor  $\kappa$ B (NF- $\kappa$ B) pathways. In the later stages of carcinogenesis, excessive ROS may counterintuitively lead to apoptosis [6, 8, 9]. Moreover, ROS continually stimulate the proliferation and survival of tumor cells by activating various transcription factors [10]. Another type of mutation associated with oxidative stress in CRC is DNA microsatellite instability (MSI), which is related to incorrect DNA repair during genome replication [9, 11].

In recent years, it has been increasingly recognized that ROS play a multifaceted role in shaping the tumor microenvironment (TME). Many preclinical studies have shown that immune checkpoint therapy (ICT) and chimeric antigen receptor (CAR)-T-cell therapy can both induce oxidative stress in the TME as well as tumor cells; meanwhile, these two therapies are vulnerable to suppression imposed by ROS derived from the surrounding immunosuppressive cells such as regulatory T cells (Tregs) and myeloid-derived suppressor cells (MDSCs). Therefore, therapeutic strategies should be developed to amplify T-cell-induced oxidative stress in cancer cells but inhibit elevated oxidative stress imposed on effector T cells by the TME [12].

Long noncoding RNAs (lncRNAs) are a class of RNA transcripts with a length greater than 200 nucleotides that have diverse biological functions in cells [13, 14]. It has been revealed that lncRNAs play an important role in tumor growth, metastasis and oxidative stress [15, 16]. For example, the lncRNAs GABPB1-AS1 and GABPB1 can regulate oxidative stress during erastin-induced ferroptosis in the hepatocellular carcinoma cell line HepG2, and high expression levels of GABPB1 are positively correlated with poor prognosis in HCC patients, while high levels of GABPB1-AS1 are correlated with improved overall survival (OS) [17]. The XIST lncRNA promotes oxidative stress-induced migration, invasion, and epithelial-to-mesenchymal transition of osteosarcoma cancer cells through the miR-153-SNAI1 axis [18]. However, the treatment potential of oxidative stress-related lncRNAs has not been explored in CRC. Investigation of oxidative stress-related lncRNAs can help us better understand

the roles of oxidative stress in CRC development and provide potential markers for prognosis prediction and targets for CRC treatment.

Currently, the most commonly used prognostic prediction system of CRC in clinical practice is the TNM staging system published by the American Joint Committee on Cancer (AJCC). Previous TNM staging systems have shown excellent performance in formulating a reasonable treatment plan according to the stage, evaluating the efficacy objectively, and judging the prognosis correctly. The traditional view is that the higher the stage is, the worse the prognosis; however, studies have found that stage IIIA patients tend to have a better prognosis than some stage II patients [19]. This suggests that traditional TNM staging has limitations in accurate prognosis prediction, and this system still suffers from the following drawbacks:

- I. The system incorporates only three indicators and uses a simple linear approach to classify patients, ignoring the objectivity of patient prognosis as a complex nonlinear phenomenon.
- II. The system can no longer accurately predict the clinical prognosis of CRC patients due to its inaccurate weighting and complex time-dependent effects.
- III. The system does not integrate newly discovered prognostic predictors for improvement, such as clinical information, pathological information, molecular markers and immune status markers of patients.

In this study, we obtained the transcriptome data and clinical information of CRC patients from The Cancer Genome Atlas (TCGA) database. We further screened the differentially expressed oxidative stress-related genes based on the oxidative stress gene set and then constructed a risk model based on these oxidative stress-related lncRNAs. We verified the effectiveness and accuracy of our model using multiple methods. In summary, this study identified multiple oxidative stress-related genes that are related to the prognosis of patients with CRC and established a risk model based on these lncRNAs that can predict prognosis effectively and accurately, providing novel insights into CRC prognosis prediction and treatment. The proposed model has several novelties compared to the previous TNM system as follows:

- I. The prognostic model based on oxidative stress shows high diagnostic accuracy, is valuable for clinical translation and was validated using an independent cohort.
- II. The model combines TMB, immune status markers and traditional pathological prognostic indicators to more accurately predict the prognosis of CRC patients.
- III. The model can guide clinicians to select the appropriate drug therapy by comparing the sensitivity of patients to common anticancer drugs in high-risk and low-risk populations.

## Results

### DEOSG identification and functional enrichment analyses

A gene list containing 789 oxidative stress-related genes was curated. Differentially expressed genes between 568 CRC samples and 44 adjacent normal tissues were

identified. As a result, 226 oxidative stress-related genes, comprising 118 down-regulated and 108 up-regulated genes, were identified as DEOSGs ( $P < 0.05$  and  $|\log_2FC| > 1.0$ ). The expression of the DEOSGs in the two subgroups is displayed in Fig. 1. To investigate the potential functional and underlying molecular mechanisms of these DEOSGs, Gene Ontology (GO) and Kyoto Encyclopedia of Genes and Genomes (KEGG) analyses were performed. KEGG analysis showed that the DEOSGs were enriched in the synapse pathway, energy metabolic pathway, drug metabolism pathway, and steroid hormone biosynthesis pathway, all of which are associated with CRC development. The top 10 enriched GO terms included response to oxidative stress, aging, secretory granule lumen, and oxidoreductase activity, acting on peroxide as acceptor (Figs. 2 and 3). All these enrichment analyses indicate that the DEOSGs are involved in metabolism and CRC progression.

### Construction and verification of a prognostic model in patients with CRC

According to univariate Cox regression analysis, we identified prognostic oxidative stress-related lncRNAs significantly correlated with OS (all  $P < 0.05$ ). To avoid over-fitting the prognostic model, we performed LASSO regression analysis on these lncRNAs. Finally, 9 lncRNAs (*AC034213.1*, *AC008124.1*, *LINC01836*, *USP30-AS1*, *AP003555.1*, *AC083906.3*, *AC008494.3*, *AC009549.1*, and *AP006621.3*) were identified that were related to oxidative stress in CRC when the first-rank value of  $\text{Log}(\lambda)$  was the minimum likelihood of deviance (Fig. 4A, B). We calculated the risk score with the following formula:

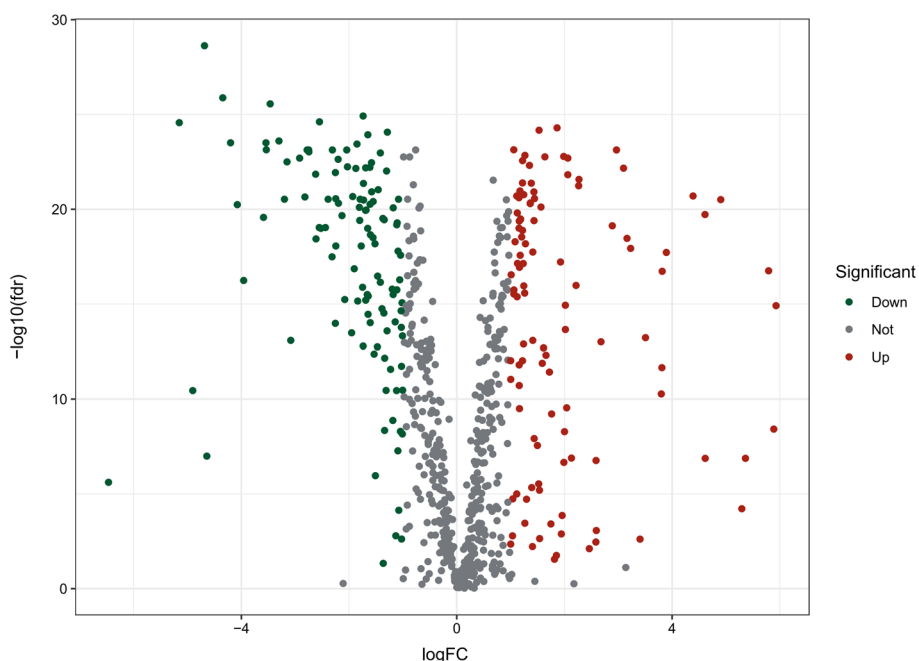


**Fig. 1** Volcano plot of DEOSGs between CRC and normal samples. Dots in green represent significantly downregulated genes, dots in red represent significantly upregulated genes, and dots in gray represent genes whose expression levels were not changed significantly

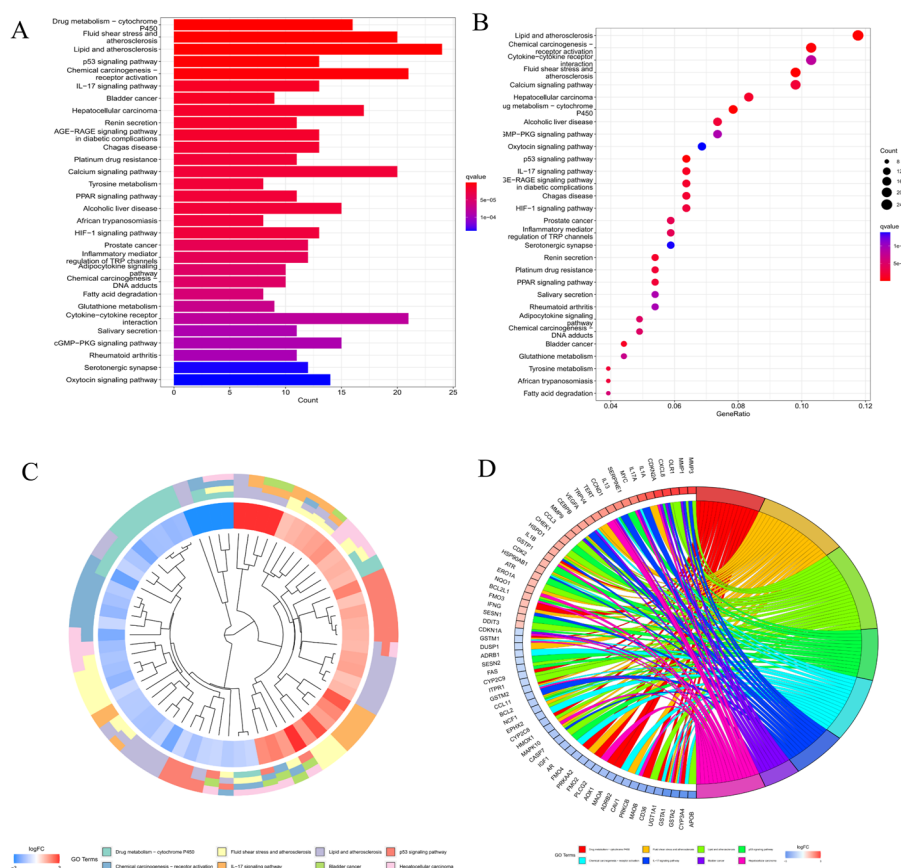


**Fig. 2** KEGG enrichment analysis of DEOSGs [20–22]. **A, B** Top 30 classes of KEGG enrichment terms. Cluster diagram (**C**) and Circle diagram (**D**) showing terms enriched in KEGG analysis

$$\begin{aligned}
 \text{Risk score} = & AC034213.1 \times (0.7704) + AC008124.1 \times (1.1086) \\
 & + LINC01836 \times (0.7098) + USP30 - AS1 \times (-0.9771) \\
 & + AP003555.1 \times (1.4298) + AC083906.3 \times (1.1536) \\
 & + AC008494.3 \times (-3.6350) + AC009549.1 \times (1.5010) \\
 & + AP006621.3 \times (0.4908)
 \end{aligned}$$

Based on the model, all patients with CRC were separated into low- and high-risk groups according to the median risk score. As shown in Fig. 4C, the OS of patients with CRC significantly decreased as the risk score increased. The number of deaths of CRC patients in the high-risk group was significantly higher than that of patients in the low-risk group (Fig. 4D, E). The heatmap shows the differential expression of 9 lncRNAs between the high- and low-risk groups (Fig. 4F). In addition, time-dependent ROC analysis indicated that the prediction model was quite credible, with the area under the ROC curve (AUC) reaching 0.703 at 5 years, indicating that this prognostic model had moderate specificity and sensitivity (Fig. 4G). This finding suggests that our risk model could predict OS not only for the total population but also for CRC patients.

To better understand the potential effect of lncRNAs on mRNAs in CRC, we built a lncRNA–mRNA network and used Cytoscape and Sankey diagrams to visualize the

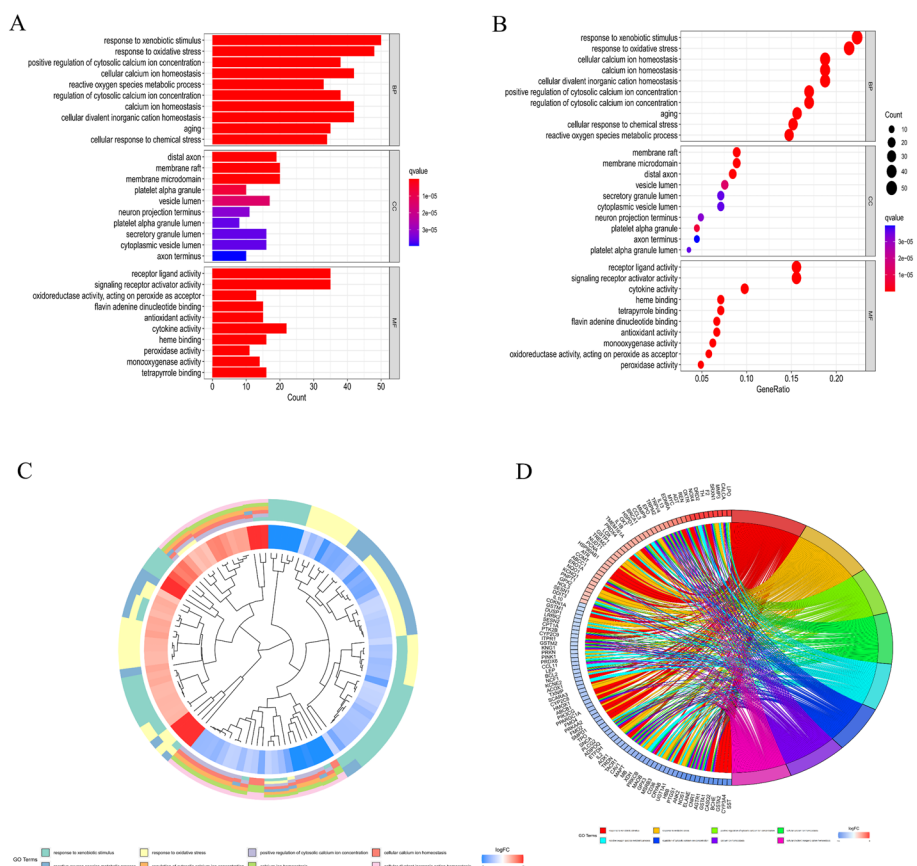


**Fig. 3** GO enrichment analysis of the DEOSGs. **A, B** Top 10 classes of GO enrichment terms in the biological process (BP), cellular component (CC), and molecular function (MF) categories. Cluster diagram (**C**) and circle diagram (**D**) showing terms enriched in GO analysis

network. We constructed the lncRNA–mRNA coexpression network using the nine screened oxidative stress-associated lncRNAs with Pearson correlation analysis ( $|R| > 0.4$  and  $P < 0.05$ ). A total of 60 lncRNA–mRNA pairs were filtered, and the correlations among lncRNAs, mRNAs, and the risk score groups were determined by the Sankey diagram (Fig. 5A, B).

Univariate and multivariate Cox regression analyses were performed to determine whether the risk score was an independent prognostic factor. Unfortunately, in univariate Cox regression analysis, although  $P < 0.05$ , the HR of the risk score was only 1.005; thus, it could not be said that the risk score was an independent prognostic factor yet. The risk score was no longer an independent prognostic factor in multivariate Cox regression analysis ( $P = 0.807$ ) (Fig. 6A, B). The ROC curve at 1 year showed that the prognostic model had better predictive accuracy than other clinical features. The ROC curve at 5 years showed that the prognostic model had better predictive performance than other factors, including age, sex, T stage, N stage, and M stage (Fig. 6C, D). In addition, the conventional clinicopathologic characteristic stage showed the same results (Fig. 6E, F). Additionally, the C-index curve showed that the C-index of the risk score was greater than 0.7, indicating that the model had moderate accuracy (Fig. 6G). A nomogram plot is another quantitative model used to predict the clinical outcomes of

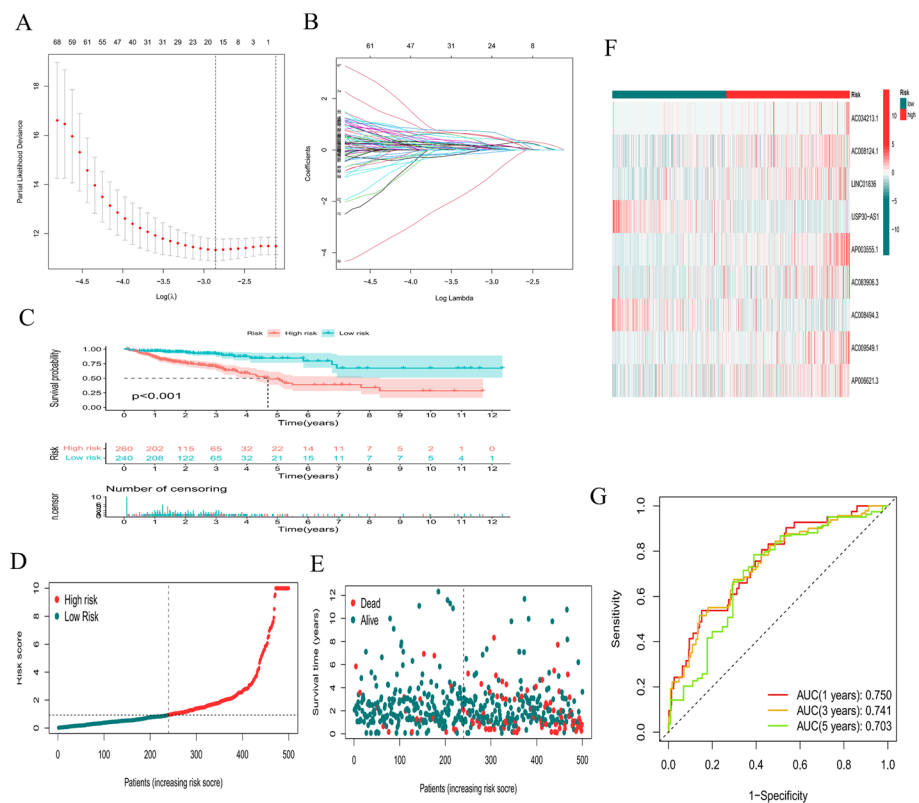


**Fig. 4** Construction of a prognostic model. **A, B** LASSO analysis for determining the number of factors and constructing the prognosis prediction model. **C** Survival curve. **D, E** Risk score distribution and survival status. **F** heatmap showing the expression levels of the 9 lncRNAs in patients in the low- and high-risk groups. **G** TimeROC curves for forecasting OS

patients with CRC. A nomogram plot was developed based on the risk score and other clinical characteristics, allowing the calculation of the survival probabilities of individual patients with CRC at 1, 3, and 5 years (Fig. 6H). The calibration plots indicated good conformity between the predicted and observed outcomes at 3 and 5 years (Fig. 6I). We also employed principal component analyses (PCAs) to demonstrate the distribution patterns of the two subgroups in two-dimensional and three-dimensional graphs (Fig. 7A–E). T-distributed stochastic neighbor embedding (t-SNE) also indicated that two risk groups could be distinguished clearly (Fig. 7F, G). These results indicated that the prognostic model is effective for predicting CRC outcomes and clinical features.

**Evaluation of the prognostic value of 9 oxidative stress-related lncRNAs in an independent gene expression omnibus (GEO) validation cohort**

To validate the prognostic value of the 9 oxidative stress-related lncRNAs, the GEO validation cohorts were divided into high- and low-expression groups. Due to the small number of CRC samples in the GEO dataset, 5 lncRNAs (*AC034213.1*, *LINC01836*, *AP003555.1*, *AC083906.3*, and *AC009549.1*) were not expressed in the GEO dataset, so we grouped the sample based on the median expression of the remaining 4 lncRNAs. Unfortunately, the survival rate of CRC patients was not statistically significant between

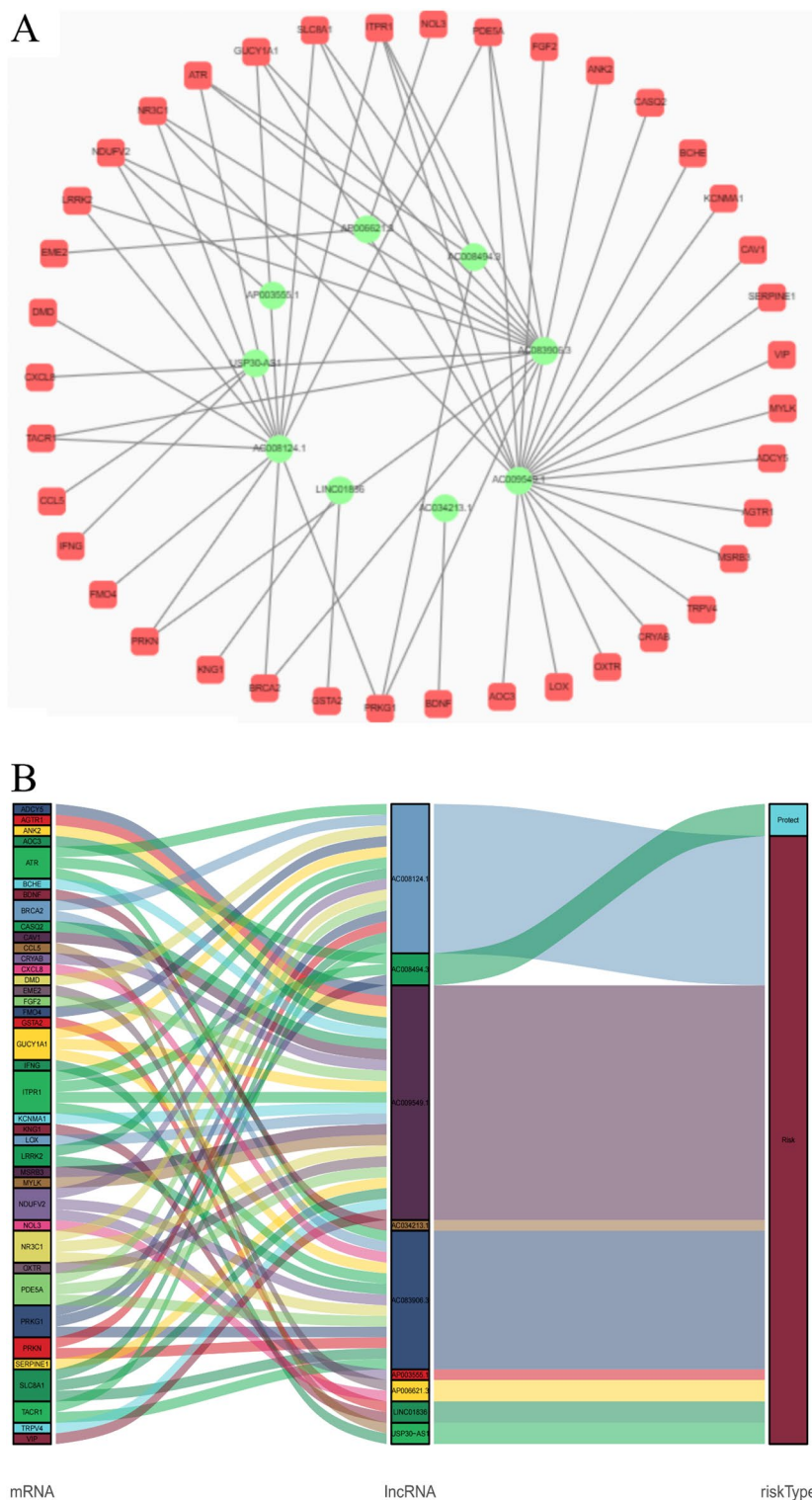


**Fig. 5** **A** The lncRNA–mRNA network between nine oxidative stress-associated lncRNAs and relevant mRNAs. Green circles indicate oxidative stress-associated lncRNAs. Red squares indicate mRNAs. The line represents a coexpression relationship between the lncRNA and the mRNA. **B** A Sankey diagram showed the co-occurrences of lncRNAs, mRNAs, and characteristics according to the risk score



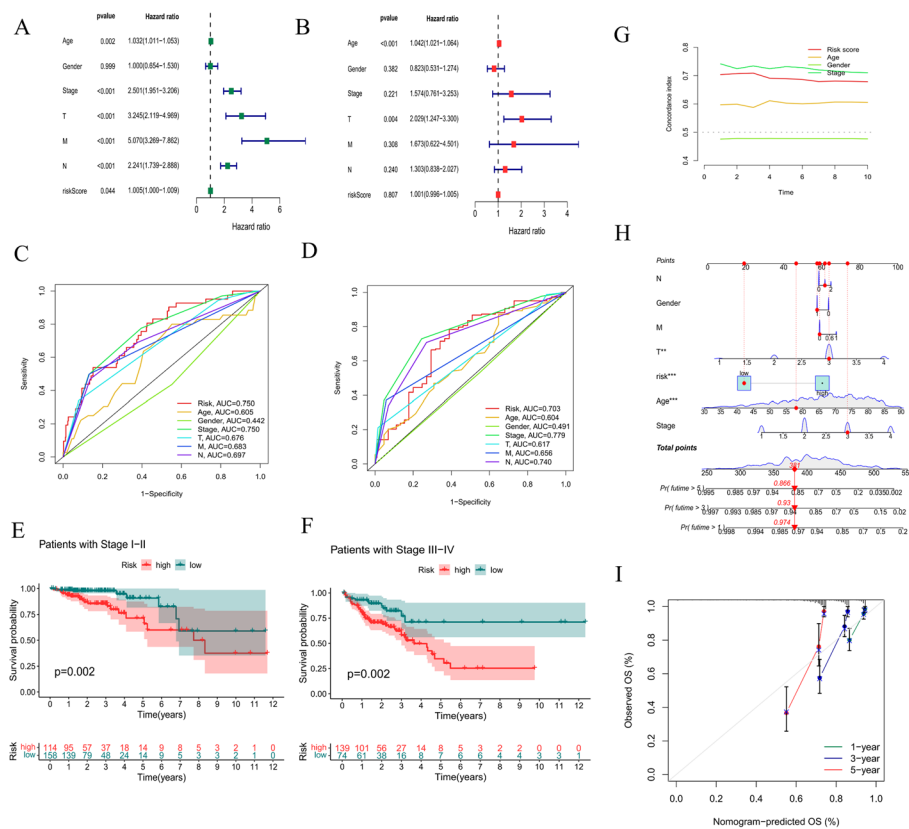


**Fig. 6** Efficacy evaluation of the constructed prognostic model. Univariate (A) and multivariate (B) Cox regression analyses of the clinicopathological features. Clinical ROC curves at 1 year (C) and 5 years (D) for forecasting overall survival. The relationship between the risk score and stage I-II (E) and stage III-IV (F). G The constructed C-index curve. H The constructed nomogram of the risk score and other clinical factors for predicting the OS of patients with CRC at 1, 3, and 5 years. I The calibration plot of the nomogram

any of the high- and low-expression groups ( $P > 0.05$ ) (Fig. 8). This is inconsistent with our previous results and may be related to the small sample size. Therefore, the exact role of these oxidative stress-related lncRNAs in CRC needs to be further investigated.

### Tumor mutation burden (TMB) analysis

It has been established that somatic mutations are a characteristic of CRC. Indeed, we found that APC, TP53, TTN, and KRAS had high mutation rates in both the low- and high-risk groups (TMB rate  $> 40\%$ ) (Fig. 9A, B). The OS of patients with CRC was significantly different among the high-TMB and high-risk, high-TMB and low-risk, low-TMB and high-risk, and low-TMB and low-risk groups ( $P < 0.001$ ) but not significantly different between the low- and high-TMB groups (Fig. 9C, D). Unexpectedly, there was no difference in TMB between the high- and low-risk groups (Fig. 9E). Additionally, a weak negative correlation was observed between the risk score and TMB ( $R = -0.013$ ) (Fig. 9F).

CRCs with microsatellite instability (MSI) have a significantly higher TMB than CRCs microsatellite stability (MSS). We regrouped the CRC samples according to the MSI score. Samples with MSI scores greater than 10 were classified as the positive group, and those that did not have MSI scores greater than 10 were classified as the negative

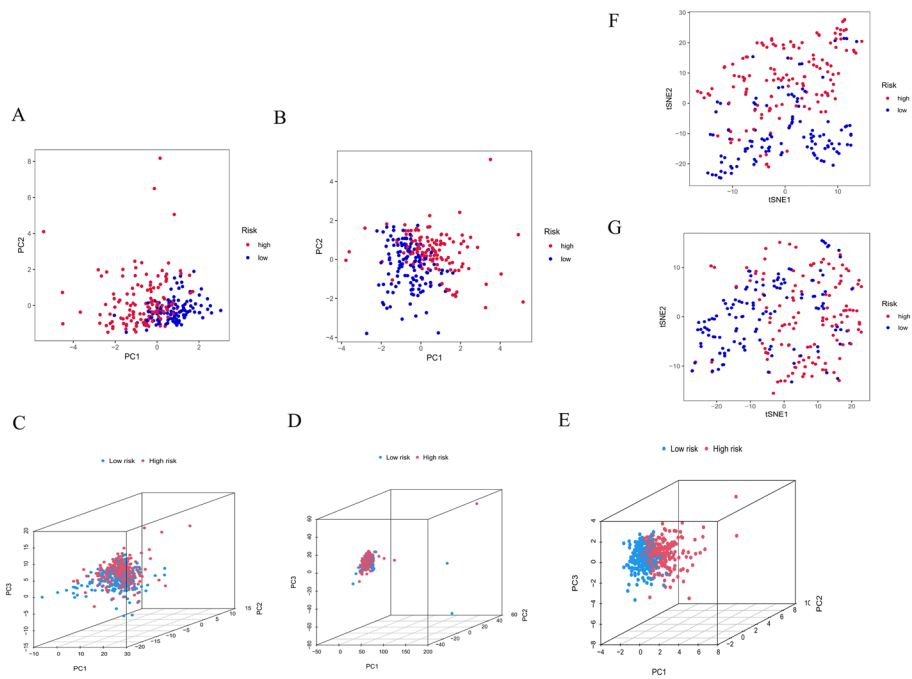


**Fig. 7** Evaluation of the efficacy of the constructed prognostic model. PCA of the risk groups in the testing (A) and training sets (B). PCA-3D of the risk groups based on all OS genes (C), DEOSGs (D), and 9 oxidative stress-related lncRNAs (E). The t-SNE of risk groups in the testing (F) and training sets (G)

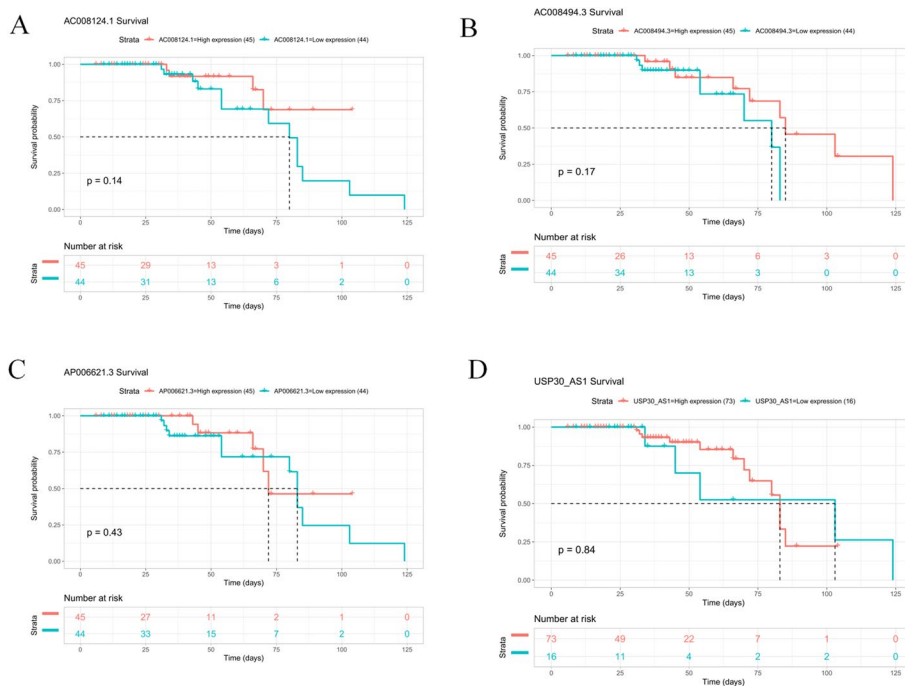


**Fig. 8** K-M survival curves for 4 target lncRNAs in CRC. The horizontal coordinate of the KM-plot is the survival time and the vertical coordinate is the survival rate. The starting point is the time of the start of follow-up, the falling curve represents patient death, and the "+" sign on the curve indicates censoring (last follow-up time for patients who are still alive)

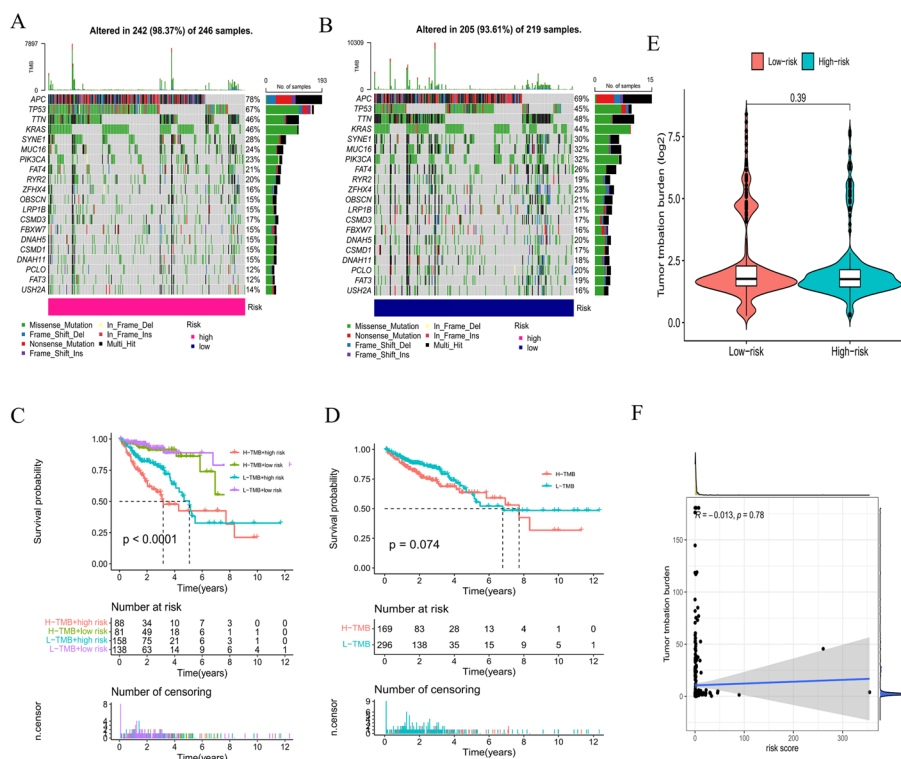


**Fig. 9** TMB analysis. The mutation rates in the high- (A) and low-risk groups (B). C–D Survival analysis of patients with different TMB levels. E Comparison of TMB for patients in the high- and low-risk groups. F Relevance analysis of TMB

group. Consistent with the results of previous studies, the low-TMB group showed a tendency toward prolonged survival ( $P < 0.001$ ) (Fig. 10A, C). However, the subsequent stratified survival analysis showed that the risk score could distinguish the survival of patients with CRC in both the MSI-positive and MSI-negative subgroups and that the trend of the survival advantage in the MSI-positive group was reversed by the risk score (Fig. 10B, D). Unfortunately, there was no difference in TMB between the high- and low-risk groups in both the MSI-positive and MSI-negative groups ( $P > 0.05$ ) (Fig. 10E, F). Inconsistently, a weak positive correlation was observed between the risk score and TMB in both the MSI-positive ( $R = 0.10$ ) and MSI-negative groups ( $R = 0.05$ ) (Fig. 10G, H).

**Gene set enrichment analysis (GSEA)**

To investigate differences in biological functions between the two subgroups, we analyzed the KEGG enriched pathways using GSEA. The top ten enriched pathways in the high- and low-risk groups were related to tumor invasion, metabolism, and immunity (Fig. 11A, B). More specifically, adherens junction, basal cell carcinoma, and the Wnt signaling pathway were primarily enriched in the high-risk group, while galactose metabolism, oxidative phosphorylation, and the proteasome were considerably enriched in the low-risk group. Therefore, we identified different enriched pathways in different subgroups by the prognostic model.

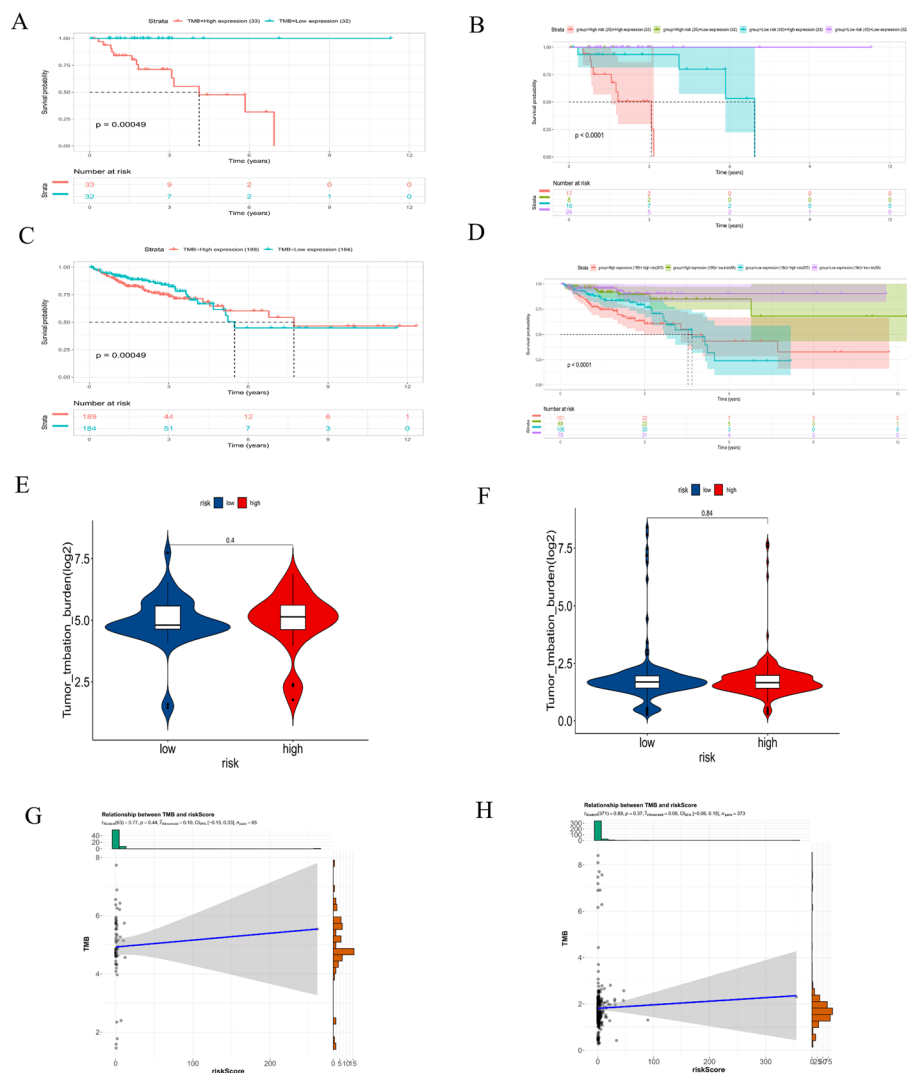


**Fig. 10** TMB analysis in the MSI-positive and MSI-negative groups. Survival analysis of patients with different TMB levels and different risk scores in the MSI-positive (**A, B**) and MSI-negative groups (**C, D**). Comparison of TMB in patients with high- and low-risk scores in the MSI-positive (**E**) and MSI-negative groups (**F**). Relevance analysis of TMB in the MSI-positive (**G**) and MSI-negative groups (**H**)

### Immune characteristics of the high- and low-risk subgroups

The TME, which is the surrounding microenvironment of tumor cells, comprises immune cells, surrounding blood vessels, fibroblasts, extracellular stroma, and various signaling molecules. We first explored the relationship between the oxidative stress-related risk score and the TME. We found that the high-risk group presented higher immune cell infiltration than the low-risk group; however, our analysis showed that the low-risk group presented a higher ESTIMATE score and lower tumor purity than the high-risk group (Fig. 12A–C).

Heatmaps were constructed, as shown in Fig. 11C, D. The CIBERSORT algorithm was applied to estimate the ratios of infiltrated immune cells in the TMEs of the high- and low-risk groups. The results revealed that the ratio of infiltrated CD8<sup>+</sup>

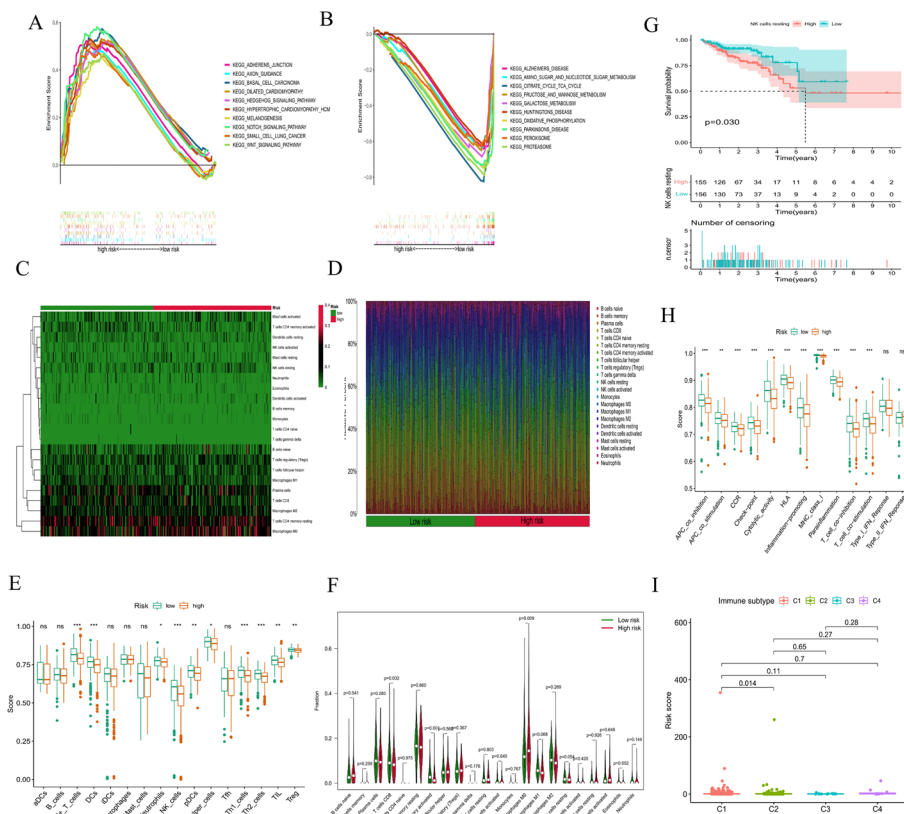


**Fig. 11** Investigation of immune cell infiltration and clinical treatment in different risk groups. GSEA of the top 10 pathways significantly enriched in the high-risk group (A) and low-risk group (B). C, D The immune cell heatmap of different risk groups. E The comparison of immune-related scores between the low- and high-risk groups. F The comparison of ratios of infiltrated immune cells between the low- and high-risk groups. G Survival curve of resting NK cells. H The comparison of immune functions between the low- and high-risk groups. I The comparison of immune subtypes between the low- and high-risk groups

T cells was notably higher in the low-risk group, while the ratios of infiltrated M0 macrophages and activated memory CD4<sup>+</sup> T cells were markedly higher in the high-risk group. Similarly, ssGSEA showed that the ratios of infiltrated CD8<sup>+</sup> T cells, dendritic cells, NK cells, TH1 cells, and TH2 cells were notably higher in the low-risk group (all  $P < 0.05$ ) (Fig. 11E, F); moreover, the ratio of infiltrated resting NK cells was closely related to the OS of patients with CRC, which was significantly worse with an increased infiltration of resting NK cells (Fig. 11G). We also found that lower risk scores were more likely to be associated with immune function, such as APC co-inhibition, CCR (C–C chemokine receptor), check point, cytolytic activity, HLA, inflammation promotion, MHC class I, parainflammation, T-cell co-inhibition and T-cell co-stimulation (Fig. 11H). We also identified 4 immune subtypes in CRC patients (C1–C4) based on their ssGSEA scores. The risk scores were significantly different between the C1 and C2 subtypes ( $P < 0.05$ ) (Fig. 11I). In summary, our results suggest that CRC patients in the low-risk group tend to have a more favorable (i.e., immune-activated) TME, while CRC patients in the high-risk group tend to have an immunosuppressive TME that can contribute to the immune escape of tumor cells and is related to a worse prognosis. Consistent with previous reports [23, 24], patients in the

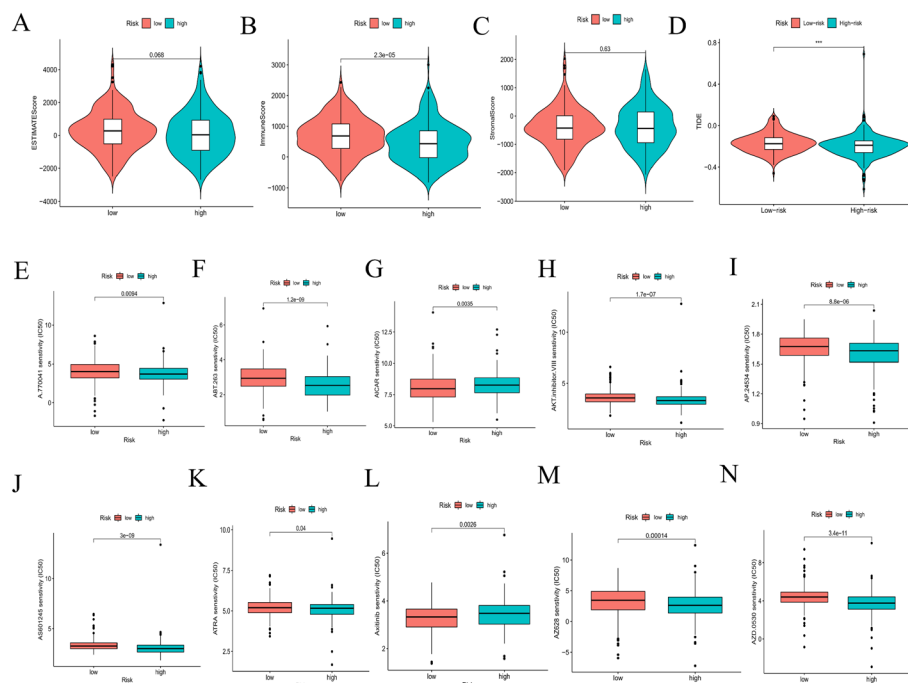


**Fig. 12** Investigation of immune cell infiltration and clinical treatment in different risk groups. **A–C** The comparison of immune-related scores between the low- and high-risk groups. **D** The comparison of the response to immunotherapy between the low- and high-risk groups. **E–N** The immunotherapy prediction of different risk groups

low-risk group also showed a better response to immunotherapy (Fig. 12D), indicating that our model could be used to select patients who are more likely to respond to ICT.

Chemotherapy drugs are the main treatment for patients with CRC. However, chemoresistance has been associated with a poor prognosis. Herein, we further predicted the chemotherapy response to common chemotherapy drugs in the two risk subgroups. The results showed that patients in the low-risk subgroup were more sensitive to AMPK inhibitors (AICAR) and tyrosine kinase inhibitors, while patients in the high-risk subgroup were more sensitive to Lck inhibitors (e.g., A.770041), Raf inhibitors (e.g., AZ628), and ATRA (Fig. 12E–N).

## Discussion

An increasing number of studies have confirmed that oxidative stress plays a crucial role in carcinogenesis and tumor treatment [25–27]. The construction of prognostic models based on public databases provides a more comprehensive clinical genetic prognostic value, and oxidative stress-based prognostic models are becoming a research hotspot for predicting the survival prognosis of different cancers [28–30]. However, the predictive value of oxidative stress-based prognostic models for the prognosis of CRC patients is still unknown and deserves further investigation. Using the transcriptome sequencing data, especially lncRNAs, and clinicopathological features of CRC obtained from TCGA, we identified and verified the 9-lncRNA prognostic signature related to OS in this study.

In the present study, 226 DEOSGs were identified based on the public TCGA database. Pathway enrichment analysis revealed that these DEOSGs were significantly correlated with the progression of several types of tumors, such as bladder, prostate, and hepatocellular carcinomas. Moreover, these DEOSGs were significantly enriched in several biological processes, including response to xenobiotic stimulus, response to oxidative stress, calcium ion homeostasis, and cellular divalent inorganic cation homeostasis, all of which have been reportedly correlated with tumorigenesis and progression [8, 31, 32]. Furthermore, we identified 2169 oxidative stress-related lncRNAs by coexpression analysis. More importantly, a total of 9 prognostic oxidative stress-related lncRNAs, i.e., *AC034213.1*, *AC008124.1*, *LINC01836*, *USP30-AS1*, *AP003555.1*, *AC083906.3*, *AC008494.3*, *AC009549.1*, and *AP006621.3*, were screened by univariate Cox and LASSO regression analyses. High expression of these 9 lncRNAs is related to good prognosis in patients with CRC. A previous study showed that *Linc01836* may serve as a valuable noninvasive biomarker for the population screening, early detection, and clinical surveillance of CRC [33]. Other studies have found that *AP0355.1* is closely associated with the poor prognosis of CRC and significantly correlated with OS, so it could be used as a promising biomarker for clinical outcome and therapeutic response predictions in colon cancer patients [34, 35]. In addition, the Sankey diagram showed that some of these lncRNAs were related to famous genes such as *ATR* and *BRCA2*. Some reports have shown that *AC008124.1* is associated with *ATR*, and *MMR* promotes a *DDR* mediated by *ATR*, a key signaling kinase, in response to various types of DNA damage, including some encountered in widely used chemotherapy regimens [11]. In addition, some studies have shown that *BRCA2* mutations are associated with CRC, but studies on how these mutations contribute to CRC development have shown conflicting results. For example, Gay-Bellile et al. [36] found that *BRCA2* variants were implicated in familial CRC inheritance; however, one meta-analysis showed that there is an increased risk of CRC in *BRCA1* but not *BRCA2* mutation carriers [37–39]. Therefore, the conclusion from this study must be validated further in future large-scale studies.

The median risk score classified the patients into two groups, and K-M curve analysis showed that patients with high risk scores had a significantly worse prognosis; moreover, the stage factors were significantly related to the risk score. There was a tendency for a higher oxidative stress-related lncRNA-based risk score to be associated with a more advanced clinical stage. However, univariate and multivariate Cox analyses confirmed that the oxidative stress-related lncRNA-based risk score was not an independent predictor of OS. In addition, we built a nomogram to predict the OS at 1, 3 and 5 years as well as the risk of death. The performance of the nomogram was highly consistent with our prognostic model. Thus, our nomogram may provide simple but accurate prognostic predictions for CRC patients.

Using different analyses, we uncovered the underlying mechanisms of different risk groups identified by our prognostic model. GSEA indicated that the low-risk group contained a higher fraction of some immune-related cells and functions. According to previous studies, the tumor immune microenvironment can influence the prognosis of CRC patients [40, 41]. To determine whether the different prognoses of patients were related to tumor cell-mediated immunity, the infiltration levels of multiple immune cells in CRC patients were evaluated by different methods, including CIBERSORT and ssGSEA. We found that

patients with high ratios of immune cell infiltration, including CD8<sup>+</sup> T cells, dendritic cells, NK cells, TH1 cells, and TH2 cells, were mostly in the low-risk subgroup. It should also be noted that CD8<sup>+</sup> T cells and NK cells favor antitumor activity in CRC and are associated with a better OS [42]. The TIDE module was used to estimate the immune function and rejection reaction of each patient. All of the above results indicate lower malignancy and potentially better immunotherapeutic effects in these patients [43, 44]. Thus, these results tentatively suggest that the poorer prognosis in the high-risk group may be due to dysregulation of antitumor immunity, and how oxidative stress affects the development of CRC through antitumor immunity still needs further study.

Moreover, the risk score was associated with TMB, suggesting that the poor prognosis of CRC patients in the high-risk group may be due to more mutated genes in this group. Increasing evidence suggests that patients with MSI-H are more sensitive to immunotherapy and can benefit from immunotherapy drugs [45]. As current immunotherapy is still in its infancy for CRC, patients with poor prognoses may benefit from immunotherapy due to their high TMB score with more mutated genes [46]. In the present study, the proportion of MSI-H patients was higher in the low-risk score group, and thus, the level of immune cell infiltration was subsequently upregulated in dMMR-MSI-H patients. Therefore, dMMR-MSI-H CRC patients may respond well to immune checkpoint blockade [47, 48]. CRC patients with MSI-H have both good and poor prognosis characteristics, and the specificity of MSI-H CRC determines the need for individualized treatment. The half maximal inhibitory concentration (IC<sub>50</sub>) was used to investigate the differences in sensitivity to common chemotherapeutic agents between the high- and low-risk groups.

In the current study, we established an oxidative stress-based prognostic model for predicting prognosis in CRC and revealed the relationship between oxidative stress-related lncRNAs and immune status. Nonetheless, there were still several limitations in our study. First, our prognostic model was constructed and validated using a TCGA cohort and requires other realistic prospective data to assess its future clinical predictive value. Second, further molecular biology experiments are needed to explore the relationship between oxidative stress and the prognostic features of CRC. Finally, the potential correlation between the risk score and antitumor immunity remains to be further investigated. Therefore, given the above limitations, the conclusions drawn from this study require more detailed validation.

## Conclusion

In summary, with a series of bioinformatic analyses, 9 oxidative stress-related lncRNAs were identified, which were related to the prognosis of patients with CRC. A prognostic model with powerful predictive ability was constructed. The relationships and underlying mechanisms among oxidative stress, lncRNAs, anti-immunity function, and CRC are worth further exploration.

## Methods

### Data acquisition and identification of differentially expressed oxidative stress-related genes (DEOSGs)

The RNA sequencing data of 568 CRC samples and 44 normal tissues, DNA mutation data of 582 CRC samples, and clinical information of 548 patients were downloaded



from the TCGA database (<https://portal.gdc.cancer.gov/>). The gene expression profile matrixes of the CRC cohort from GSE192667 were downloaded from the GEO website (<https://www.ncbi.nlm.nih.gov/geo/>) for validation. To identify DEOSGs, we first curated a gene list containing 789 oxidative stress-related genes with a relevance score  $\geq 7$  on the GeneCards website (<https://www.genecards.org>) (Additional file 1), followed by transcriptional analysis with the limma package. The oxidative stress-related genes with a false discovery rate (FDR)  $< 0.05$  and  $|\log_2\text{-fold change (FC)}| \geq 1$  were identified as DEOSGs [49]. As a result, 226 DEOSGs were included for further analyses using the Wilcox.test.

#### GO and KEGG pathway enrichment analyses

GO and KEGG pathway enrichment analyses were performed for the 226 DEOSGs, and the results were visualized using the clusterProfiler package (version 4.1.3) [50, 51]. Of note, GO analyses included biological process (BP), cellular component (CC), and molecular function (MF) analyses. A *P* value and adjusted *P* (q) value smaller than 0.05 were considered statistically significant.

#### Selection of oxidative stress-related lncRNAs

A total of 16,773 lncRNAs were identified in the raw transcriptome data using Strawberry Perl and the limma package [52, 53]. Correlation analysis was performed between the expression of 226 DEOSGs (Additional file 2) and 16,773 lncRNAs. lncRNAs with Pearson correlation coefficients  $> 0.4$  and  $P < 0.001$  were selected. As a result, 2169 lncRNAs were identified as oxidative stress-related lncRNAs.

#### Construction of the coexpression network

To better understand the relationship between lncRNAs and mRNAs, the lncRNA–mRNA coexpression network was visualized by Cytoscape software (<http://www.cytoscape.org/>).

#### Construction and validation of the prognostic model

To reduce statistical bias in the analysis, CRC patients with missing OS data or with short OS values ( $< 30$  days) were excluded. Finally, we retrieved transcriptome, mutation, and clinical data for 506 patients. These patients were randomly grouped into the training and testing groups at a ratio of 1:1 using Strawberry Perl and the caret package. All oxidative stress-related lncRNAs were subjected to univariate Cox regression analyses to explore the relationship between lncRNA expression and patient OS by the survival package. lncRNAs with a  $P < 0.05$  were identified as prognostic oxidative stress-related lncRNAs. Subsequently, these candidate lncRNAs were integrated into least absolute shrinkage and selection operator (LASSO) regression to construct a prognostic model [54]. The risk score of each patient was calculated with the following formula:

$$\text{Risk score} = \sum_{n=1}^k \text{expr} - (\ln \text{cRNA}) * \beta_i$$

where  $\text{expr}(\text{lncRNA})$  represents the short form of the expression of lncRNAs correlated with survival and  $\beta_i$  represents the regression coefficient.

The CRC patients were grouped into low- and high-risk subgroups based on the median risk score [52, 55]. The Kaplan–Meier method and log-rank test using the R Bioconductor survival package were further conducted to compare OS [56, 57]. Scatter plots were used to display the survival status of CRC patients in the low- and high-risk groups. Utilizing the pheatmap package, a heatmap was constructed to show the differential expression of 9 lncRNAs between the low- and high-risk groups. The effectiveness and accuracy of the model were further verified using the survival and timeROC packages [58]. Univariate and multivariate Cox regression analyses were also performed to evaluate the relationship between clinical characteristics and the risk score. Additionally, a concordance index (C-index) curve was constructed to evaluate the prediction accuracy of the model in CRC patients using the pec package [59]. Risk score, age, sex, and tumor stage were used to construct a nomogram for predicting 1-, 2-, and 3-year OS using the rms package. Correction curves based on the Hosmer Lemeshow test showed that the predicted prognosis was in good agreement with the actual outcome [60, 61]. Finally, PCA and t-SNE were performed by the Rtsne and scatterplot3d packages to determine whether two subgroups could be distinguished by these two metrics [62, 63].

#### **Evaluation of the prognostic value of 9 oxidative stress-related lncRNAs in an independent GEO validation cohort**

The CRC patients in GEO were grouped into low and high expression subgroups based on the median level of the lncRNAs [64]. The Kaplan–Meier method using the R Bioconductor survival package was further conducted to compare the OS between the two subgroups, and then the survival and survminer packages were used to plot the survival curves.

#### **TMB analysis**

The DNA mutation data of CRC patients were downloaded from the TCGA database. The mutation rates in the high- and low-risk groups were visualized using the maftools and Rhtslib packages. Differences regarding TMB and OS in the high- and low-risk groups were analyzed using the limma, ggpubr, and survivor packages [65]. A relevance analysis between the risk scores and TMBs was performed using the limma, ggpubr, and ggExtra packages.

We further downloaded the reference list of MSI scores from the cBioPortal database (<https://www.cbioportal.org/>) (Additional file 3) [66]. Samples with MSI scores greater than 10 were classified as the positive group, and those with MSI scores not greater than 10 were classified as the negative group. In the MSI-positive and MSI-negative groups, the ggplot2, survivor and ggstatsplot packages were used to perform difference analysis, survival analysis and correlation analysis between TMB and the risk score [67, 68].

#### **GSEA**

GSEA (<https://www.gsea-msigdb.org/gsea/login.jsp>) was performed using the “kegg.v7.4.symbols.gmt” gene set to identify significantly enriched pathways between the

low- and high-risk groups. Pathways with  $P < 0.05$  and  $FDR < 0.25$  were regarded as significantly enriched pathways [29].

### Analyses of TME and immune cell infiltration

The ESTIMATE scores, immune scores, and stromal scores of CRC samples were estimated based on transcriptional data using the “estimation of stromal and immune cells in malignant tumors using expression data” (ESTIMATE) method [69]. Tumor purity was inferred based on the *ggpubr* package. Moreover, the abundances of 22 tumor-infiltrating immune cells were estimated using the “cell-type identification by estimating relative subsets of RNA transcripts” (CIBERSORT) algorithm [70]. Utilizing the *limma*, *ggpubr*, *pheatmap* and *vioplot* packages, a heatmap was constructed to show the differential expression of immune cells between the low- and high-risk groups and the relative expression of immune cells in each sample. Immune cell infiltration was also estimated using single-sample GSEA (ssGSEA) [71, 72]. To assess the effectiveness of our model in predicting immunotherapy response, the online tool, Tumor Immune Dysfunction and Exclusion (TIDE) (<http://tide.dfci.harvard.edu/>), was used to estimate patient response to immune checkpoint therapy.

### Exploration of the model in clinical treatment

The clinical responses of CRC patients to different chemotherapy drugs were predicted using the *pRRophetic* package. We compared the half-maximal inhibitory concentration (IC50) between the high- and low-subgroups [73].

### Abbreviations

AMPK	Adenosine 5'-monophosphate (AMP)-activated protein kinase
Akt	(PKB) protein kinase B
APC	Antigen-presenting cell
ATR	ATM and Rad3-related
ATRA	All-trans retinoic acid
ATM	Ataxia telangiectasia mutated
AUC	Area under the ROC curve
BP	Biological process
CAR-T	Chimeric antigen receptor T-cell immunotherapy
CC	Cellular component
CCR	C-C chemokine receptor
CIBERSORT	Cell-type identification by estimating relative subsets of RNA transcripts
CRC	Colorectal cancer
DDR	DNA damage response
DEOSGs	Differentially expressed oxidative stress-related genes
dMMR-MSI-H	Mismatch repair deficient high microsatellite instability
ESTIMATE	Estimation of stromal and immune cells in malignant tumors using expression data
FDR	False discovery rate
GEO	Gene expression omnibus
GO	Gene ontology
GSEA	Gene set enrichment analysis
HLA	Human leukocyte antigen
IC50	Half-maximal inhibitory concentration
ICT	Immune-checkpoint therapy
JNK	C-junN-terminal kinase
KEGG	Kyoto encyclopedia of genes and genomes
LASSO	Least absolute shrinkage and selection operator
Lck	Lymphocyte-specific protein tyrosine kinase
MDSCs	Myeloid-derived suppressor cells
MF	Molecular function
MHC	Major histocompatibility complex
MMR	Mismatch repair
MSI	Microsatellite instability

MSS	Microsatellite stability
multi-Cox	Multivariate Cox regression
NF-κB	Nuclear factor κB
OS	Overall survival
PCA	Principal component analysis
PI3K	Phosphatidylinositol 3-kinase
ROC	Receiver operating characteristic
ROS	Reactive oxygen species
RTK	Receptor tyrosine kinase
ssGSEA	Single-sample gene set enrichment analysis
TCGA	The cancer genome atlas
TIDE	Tumor immune dysfunction and exclusion
TMB	Tumor mutation burden
TME	Tumor environment
Tregs	Regulatory T cells
t-SNE	T-distributed stochastic neighbor embedding

## Supplementary Information

The online version contains supplementary material available at <https://doi.org/10.1186/s12859-023-05203-5>.

**Additional file 1.** The List of 789 oxidative stress-related genes.

**Additional file 2.** The List of 226 differentially expressed oxidative stress-related genes.

**Additional file 3.** The reference list of MSI scores.

## Acknowledgements

We would like to thank all the patients who participated in TCGA studies. We sincerely thank Dr. Jing Gong (Department of International Agency for Research on Cancer, Shandong University), Dr. Chuxiong Gong (Bioinformatics Research Institution, Chengdu, China) and Mr. Haitao Han (The First Clinical College of Shandong University) for their help in data analysis.

## Author contributions

JMW and RC designed the study, RC performed the statistical analyses and wrote the manuscript, and JMW provided a critical review. Both authors read and approved the final manuscript.

## Funding

This work was supported by the Shandong Provincial Natural Science Foundation of China (ZR2019MH122) and the Wu Jieping Medical Foundation (320.6750.2020-01-31).

## Availability of data and materials

The datasets used for analyses in the current study are available from the corresponding author upon reasonable request.

## Declarations

### Ethics approval and consent to participate

Not applicable.

### Consent for publication

Not applicable.

### Competing interests

The authors have declared that no conflict of interest exists.

Received: 9 September 2022 Accepted: 23 February 2023

Published online: 03 March 2023

## References

1. Biller LH, Schrag D. Diagnosis and treatment of metastatic colorectal cancer: a review. *JAMA*. 2021;325(7):669–85.
2. Van Cutsem E, Cervantes A, Nordlinger B, Arnold D. Metastatic colorectal cancer: ESMO Clinical Practice Guidelines for diagnosis, treatment and follow-up. *Annals Oncol Off J European Soc Med Oncol*. 2014;iii1–9.
3. Johdi NA, Sukor NF. Colorectal cancer immunotherapy: options and strategies. *Front Immunol*. 2020;11:1624.
4. Dekker E, Tanis PJ, Vieugels JLA, Kasi PM, Wallace MB. Colorectal cancer. *Lancet*. 2019;394(10207):1467–80.
5. Lin S, Li Y, Zamyatnin A, Werner J, Bazhin A. Reactive oxygen species and colorectal cancer. *J Cell Physiol*. 2018;233(7):5119–32.
6. Zhou L, Zhang Z, Huang Z, Nice E, Zou B, Huang C. Revisiting cancer hallmarks: insights from the interplay between oxidative stress and non-coding RNAs. *Mol Biomed*. 2020;1(1):4.

7. Pais R, Dumitraşcu D. Do antioxidants prevent colorectal cancer? A meta-analysis. *Romanian J Internal Med Revue Roumaine de Medecine Interne*. 2013;51:152–63.
8. D'Souza LC, Mishra S, Chakraborty A, Shekher A, Sharma A, Gupta SC. Oxidative stress and cancer development: are noncoding RNAs the missing links? *Antioxid Redox Signal*. 2020;33(17):1209–29.
9. Carini F, Mazzola M, Rappa F, Jurjus A, Geagea AG, Al Kattar S, et al. Colorectal carcinogenesis: role of oxidative stress and antioxidants. *Anticancer Res*. 2017;37(9):4759–66.
10. Saud S, Li W, Morris N, Matter M, Colburn N, Kim Y, et al. Resveratrol prevents tumorigenesis in mouse model of Kras activated sporadic colorectal cancer by suppressing oncogenic Kras expression. *Carcinogenesis*. 2014;35(12):2778–86.
11. Li Z, Pearlman AH, Hsieh P. DNA mismatch repair and the DNA damage response. *DNA Repair*. 2016;38:94–101.
12. Aboeella NS, Brandle C, Kim T, Ding ZC, Zhou G. Oxidative stress in the tumor microenvironment and its relevance to cancer immunotherapy. *Cancers*. 2021;13(5).
13. Chi Y, Wang D, Wang J, Yu W, Yang J. Long non-coding RNA in the pathogenesis of cancers. *Cells*. 2019;8(9).
14. Tehrani SS, Karimian A, Parsian H, Majidinia M, Yousefi B. Multiple functions of long non-coding RNAs in oxidative stress, DNA damage response and cancer progression. *J Cell Biochem*. 2018;119(1):223–36.
15. Huo N, Cong R, Sun ZJ, Li WC, Zhu X, Xue CY, et al. STAT3/LINC00671 axis regulates papillary thyroid tumor growth and metastasis via LDHA-mediated glycolysis. *Cell Death Dis*. 2021;12(9):799.
16. Xiu B, Chi Y, Liu L, Chi W, Zhang Q, Chen J, et al. LINC02273 drives breast cancer metastasis by epigenetically increasing AGR2 transcription. *Mol Cancer*. 2019;18(1):187.
17. Qi W, Li Z, Xia L, Dai J, Zhang Q, Wu C, et al. LncRNA GABPB1-AS1 and GABPB1 regulate oxidative stress during erastin-induced ferroptosis in HepG2 hepatocellular carcinoma cells. *Sci Rep*. 2019;9(1):16185.
18. Wen JF, Jiang YQ, Li C, Dai XK, Wu T, Yin WZ. LncRNA-XIST promotes the oxidative stress-induced migration, invasion, and epithelial-to-mesenchymal transition of osteosarcoma cancer cells through miR-153-SNAI1 axis. *Cell Biol Int*. 2020;44(10):1991–2001.
19. Kim MJ, Jeong SY, Choi SJ, Ryoo SB, Park JW, Park KJ, et al. Survival paradox between stage IIB/C (T4N0) and stage IIIA (T1–2N1) colon cancer. *Ann Surg Oncol*. 2015;22(2):505–12.
20. Kanehisa M, Goto S. KEGG: Kyoto encyclopedia of genes and genomes. *Nucleic Acids Res*. 2000;28(1):27–30.
21. Kanehisa M. Toward understanding the origin and evolution of cellular organisms. *Protein Sci*. 2019;28(11):1947–51.
22. Kanehisa M, Furumichi M, Sato Y, Kawashima M, Ishiguro-Watanabe M. KEGG for taxonomy-based analysis of pathways and genomes. *Nucleic Acids Res*. 2023;51(D1):D587–92.
23. Galon J, Costes A, Sanchez-Cabo F, Kirilovsky A, Mlecnik B, Lagorce-Pagès C, et al. Type, density, and location of immune cells within human colorectal tumors predict clinical outcome. *Science*. 2006;313(5795):1960–4.
24. Picard E, Verschoor CP, Ma GW, Pawelec G. Relationships between immune landscapes, genetic subtypes and responses to immunotherapy in colorectal cancer. *Front Immunol*. 2020;11:369.
25. Jelic MD, Mandic AD, Maricic SM, Srdjenovic BU. Oxidative stress and its role in cancer. *J Cancer Res Ther*. 2021;17(1):22–8.
26. Kalinina EV, Gavriluk LA, Pokrovsky VS. Oxidative stress and redox-dependent signaling in prostate cancer. *Biochemistry*. 2022;87(5):413–24.
27. Kuo CL, Ponneri Babuhasankar A, Lin YC, Lien HW, Lo YK, Chou HY, et al. Mitochondrial oxidative stress in the tumor microenvironment and cancer immunoescape: foe or friend? *J Biomed Sci*. 2022;29(1):74.
28. Wu Z, Wang L, Wen Z, Yao J. Integrated analysis identifies oxidative stress genes associated with progression and prognosis in gastric cancer. *Sci Rep*. 2021;11(1):3292.
29. Dong C, Zhang N, Zhang L. The multi-omic prognostic model of oxidative stress-related genes in acute myeloid Leukemia. *Front Genet*. 2021;12: 722064.
30. Zhang M, Du G, Li Z, Li D, Li W, Li H, et al. An oxidative stress-related genes signature for predicting survival in bladder cancer: based on TCGA database and bioinformatics. *Int J Gen Med*. 2022;15:2645–67.
31. Gunes-Bayir A, Kocyigit A, Guler EM, Dadak A. In vitro hormetic effect investigation of thymol on human fibroblast and gastric adenocarcinoma cells. *Molecules*. 2020;25(14):3270.
32. Guo H, Zeng W, Feng L, Yu X, Li P, Zhang K, et al. Integrated transcriptomic analysis of distance-related field cancerization in rectal cancer patients. *Oncotarget*. 2017;8(37):61107–17.
33. Shen L, Zong W, Feng W, Chen E, Ma S, Yuan J, et al. Upregulated Linc01836 in serum promisingly serving as a diagnostic and prognostic biomarker for colorectal cancer. *Front Pharmacol*. 2022;13: 840391.
34. Li N, Shen J, Qiao X, Gao Y, Su HB, Zhang S. Long non-coding RNA signatures associated with ferroptosis predict prognosis in colorectal cancer. *Int J Gen Med*. 2022;15:33–43.
35. Wu Z, Lu Z, Li L, Ma M, Long F, Wu R, et al. Identification and validation of ferroptosis-related LncRNA signatures as a novel prognostic model for colon cancer. *Front Immunol*. 2021;12: 783362.
36. Gay-Bellile M, Privat M, Martins A, Caputo SM, Pebrel-Richard C, Cavaille M, et al. Is BRCA2 involved in early onset colorectal cancer risk? *Clin Genet*. 2020;97(4):668–9.
37. Sopik V, Phelan C, Cybulski C, Narod SA. BRCA1 and BRCA2 mutations and the risk for colorectal cancer. *Clin Genet*. 2015;87(5):411–8.
38. Oh M, McBride A, Yun S, Bhattacharjee S, Slack M, Martin JR, et al. BRCA1 and BRCA2 gene mutations and colorectal cancer risk: systematic review and meta-analysis. *J Natl Cancer Inst*. 2018;110(11):1178–89.
39. Zheng L, Zhan Y, Lu J, Hu J, Kong D. A prognostic predictive model constituted with gene mutations of APC, BRCA2, CDH1, SMO, and TSC2 in colorectal cancer. *Ann Transl Med*. 2021;9(8):680.
40. Zaborowski AM, Winter DC, Lynch L. The therapeutic and prognostic implications of immunobiology in colorectal cancer: a review. *Br J Cancer*. 2021;125(10):1341–9.
41. Zhang Y, Xu J, Zhang N, Chen M, Wang H, Zhu D. Targeting the tumour immune microenvironment for cancer therapy in human gastrointestinal malignancies. *Cancer Lett*. 2019;458:123–35.
42. Fionda C, Scarno G, Stabile H, Molfetta R, Di Censo C, Gismondi A, et al. NK cells and other cytotoxic innate lymphocytes in colorectal cancer progression and metastasis. *Int J Mol Sci*. 2022;23(14):7859.
43. Wang L, Cho KB, Li Y, Tao G, Xie Z, Guo B. Long noncoding RNA (lncRNA)-mediated competing endogenous RNA networks provide novel potential biomarkers and therapeutic targets for colorectal cancer. *Int J Mol Sci*. 2019;20(22):5758.

44. Liu S, Cao Q, An G, Yan B, Lei L. Identification of the 3-lncRNA signature as a prognostic biomarker for colorectal cancer. *Int J Mol Sci.* 2020;21(24):9359.
45. Ganesh K, Stadler ZK, Cercek A, Mendelsohn RB, Shia J, Segal NH, et al. Immunotherapy in colorectal cancer: rationale, challenges and potential. *Nat Rev Gastroenterol Hepatol.* 2019;16(6):361–75.
46. Chan TA, Yarchoan M, Jaffee E, Swanton C, Quezada SA, Stenzinger A, et al. Development of tumor mutation burden as an immunotherapy biomarker: utility for the oncology clinic. *Ann Oncol.* 2019;30(1):44–56.
47. Popat S, Hubner R, Houlston RS. Systematic review of microsatellite instability and colorectal cancer prognosis. *J Clin Oncol.* 2005;23(3):609–18.
48. Llosa NJ, Cruise M, Tam A, Wicks EC, Hechenbleikner EM, Taube JM, et al. The vigorous immune microenvironment of microsatellite instable colon cancer is balanced by multiple counter-inhibitory checkpoints. *Cancer Discov.* 2015;5(1):43–51.
49. Ye Z, Zhang H, Kong F, Lan J, Yi S, Jia W, et al. Comprehensive analysis of alteration landscape and its clinical significance of mitochondrial energy metabolism pathway-related genes in lung cancers. *Oxid Med Cell Longev.* 2021;2021:9259297.
50. Chen L, Zhang YH, Wang S, Zhang Y, Huang T, Cai YD. Prediction and analysis of essential genes using the enrichments of gene ontology and KEGG pathways. *PLoS ONE.* 2017;12(9): e0184129.
51. Kanehisa M, Furumichi M, Tanabe M, Sato Y, Morishima K. KEGG: new perspectives on genomes, pathways, diseases and drugs. *Nucleic Acids Res.* 2017;45(D1):D353–61.
52. Meng T, Huang R, Zeng Z, Huang Z, Yin H, Jiao C, et al. Identification of prognostic and metastatic alternative splicing signatures in kidney renal clear cell carcinoma. *Front Bioeng Biotechnol.* 2019;7:270.
53. Zhao Z, Liu H, Zhou X, Fang D, Ou X, Ye J, et al. Necroptosis-related lncRNAs: predicting prognosis and the distinction between the cold and hot tumors in gastric cancer. *J Oncol.* 2021;2021:6718443.
54. Xiang S, Li J, Shen J, Zhao Y, Wu X, Li M, et al. Identification of prognostic genes in the tumor microenvironment of hepatocellular carcinoma. *Front Immunol.* 2021;12: 653836.
55. Hong W, Liang L, Gu Y, Qi Z, Qiu H, Yang X, et al. Immune-Related lncRNA to construct novel signature and predict the immune landscape of human hepatocellular carcinoma. *Mol Ther Nucleic Acids.* 2020;22:937–47.
56. Wu M, Li X, Zhang T, Liu Z, Zhao Y. Identification of a nine-gene signature and establishment of a prognostic nomogram predicting overall survival of pancreatic cancer. *Front Oncol.* 2019;9:996.
57. Karasinska JM, Topham JT, Kalloger SE, Jang GH, Denroche RE, Culibrk L, et al. Altered gene expression along the glycolysis-cholesterol synthesis axis is associated with outcome in pancreatic cancer. *Clin Cancer Res.* 2020;26(1):135–46.
58. Hong Y, Lin M, Ou D, Huang Z, Shen P. A novel ferroptosis-related 12-gene signature predicts clinical prognosis and reveals immune relevancy in clear cell renal cell carcinoma. *BMC Cancer.* 2021;21(1):831.
59. Yang Z, Zi Q, Xu K, Wang C, Chi Q. Development of a macrophages-related 4-gene signature and nomogram for the overall survival prediction of hepatocellular carcinoma based on WGCNA and LASSO algorithm. *Int Immunopharmacol.* 2021;90: 107238.
60. Shi H, Yu L, Mai J, Zhang P, Fang K. Nomograms predicting overall survival and cancer-specific survival in metaplastic breast cancer patients. *J Buon.* 2021;26(4):1386–97.
61. Wang Z, Gao L, Guo X, Feng C, Lian W, Deng K, et al. Development and validation of a nomogram with an autophagy-related gene signature for predicting survival in patients with glioblastoma. *Aging.* 2019;11(24):12246–69.
62. Li Y, Gu J, Xu F, Zhu Q, Ge D, Lu C. Transcriptomic and functional network features of lung squamous cell carcinoma through integrative analysis of GEO and TCGA data. *Sci Rep.* 2018;8(1):15834.
63. He D, Cai L, Huang W, Weng Q, Lin X, You M, et al. Prognostic value of fatty acid metabolism-related genes in patients with hepatocellular carcinoma. *Aging.* 2021;13(13):17847–63.
64. He L, Chen J, Xu F, Li J, Li J. Prognostic implication of a metabolism-associated gene signature in lung adenocarcinoma. *Mol Ther Oncolytics.* 2020;19:265–77.
65. Liu Z, Mi M, Li X, Zheng X, Wu G, Zhang L. A lncRNA prognostic signature associated with immune infiltration and tumour mutation burden in breast cancer. *J Cell Mol Med.* 2020;24(21):12444–56.
66. Huang D, Shen J, Zhai L, Chen H, Fei J, Zhu X, et al. Insights into the prognostic value and immunological role of NAAA in pan-cancer. *Front Immunol.* 2021;12: 812713.
67. Liu S, Xie X, Lei H, Zou B, Xie L. Identification of key circRNAs/lncRNAs/miRNAs/mRNAs and pathways in preeclampsia using bioinformatics analysis. *Med Sci Monit.* 2019;25:1679–93.
68. Xu Z, Wang S, Ren Z, Gao X, Xu L, Zhang S, et al. An integrated analysis of prognostic and immune infiltrates for hub genes as potential survival indicators in patients with lung adenocarcinoma. *World J Surg Oncol.* 2022;20(1):99.
69. Yoshihara K, Shahmoradgoli M, Martinez E, Vegesna R, Kim H, Torres-Garcia W, et al. Inferring tumour purity and stromal and immune cell admixture from expression data. *Nat Commun.* 2013;4:2612.
70. Newman AM, Liu CL, Green MR, Gentles AJ, Feng W, Xu Y, et al. Robust enumeration of cell subsets from tissue expression profiles. *Nat Methods.* 2015;12(5):453–7.
71. Bindea G, Mlecnik B, Tosolini M, Kirilovsky A, Waldner M, Obenauf AC, et al. Spatiotemporal dynamics of intratumoral immune cells reveal the immune landscape in human cancer. *Immunity.* 2013;39(4):782–95.
72. Barbie DA, Tamayo P, Boehm JS, Kim SY, Moody SE, Dunn IF, et al. Systematic RNA interference reveals that oncogenic KRAS-driven cancers require TBK1. *Nature.* 2009;462(7269):108–12.
73. Geeleher P, Cox NJ, Huang RS. Clinical drug response can be predicted using baseline gene expression levels and in vitro drug sensitivity in cell lines. *Genome Biol.* 2014;15(3):R47.

## Publisher's Note

Springer Nature remains neutral with regard to jurisdictional claims in published maps and institutional affiliations.